

ARTICLE

Received 30 Jun 2014 | Accepted 12 May 2015 | Published 23 Jun 2015

DOI: 10.1038/ncomms8476

Zic1 controls placode progenitor formation non-cell autonomously by regulating retinoic acid production and transport

Maria Belen Jaurena¹, Hugo Juraver-Geslin¹, Arun Devotta¹ & Jean-Pierre Saint-Jeannet¹

All cranial placode progenitors arise from a common precursor field anterior to the neural plate, the pre-placodal region (PPR). We showed that transcription factor Zic1, expressed at the anterior neural plate, is necessary and sufficient to promote placode fate. Here we reveal the non-cell autonomous activity of Zic1 and implicate retinoic acid (RA) signalling as a key player in cranial placode progenitor specification. In a screen for genes activated by Zic1, we identify several factors involved in RA metabolism and function. Among them we show that retinaldehyde dehydrogenase 2 (RALDH2) and lipocalin-type prostaglandin D2 synthase (LPGDS), which, respectively, regulate the synthesis and transport of RA, directly participate in the establishment of the PPR. We propose that RALDH2 and LPGDS induction by Zic1 at the anterior neural plate allows for the localized production and transport of RA, which in turn activates a cranial placode developmental programme in neighbouring cells.

¹Department of Basic Science and Craniofacial Biology, New York University, College of Dentistry, 345 East 24th street, New York, New York 10010, USA. Correspondence and requests for materials should be addressed to J.-P.S.-J. (email: jsj4@nyu.edu).

Cranial sensory placodes are thickenings of the embryonic head ectoderm that give rise to the specialized paired sense organs and sensory cranial ganglia. While they produce very diverse cell types such as sensory neurons, lens fibres and hormone-secreting cells^{1–3}, all placode progenitors arise from a common precursor field that borders the anterior neural plate known as the pre-placodal region (PPR). Subsequently, in response to inductive interactions with surrounding tissues the PPR divides into territories with distinct identities to generate the adenohipophyseal, olfactory, lens, trigeminal, otic and epibranchial placodes.

Placode progenitors are induced by a combination of inductive signals primarily mediated by fibroblast growth factor (FGF) and attenuation of bone morphogenetic protein (BMP) and Wnt signals^{4–6}. The zinc-finger transcription factor, *Zic1*, is one of the earliest genes activated in response to these signalling events, and in *Xenopus*, *Zic1* is both necessary and sufficient to promote placodal fate by regulating the expression of the PPR-specific genes, *Six1* and *Eya1* (ref. 7). Interestingly, *Zic1* is expressed at the anterior neural plate but does not overlap with the prospective PPR^{8,9}, suggesting that *Zic1* regulates placode formation in a non-cell autonomous manner. To gain insights into the mechanisms by which *Zic1* regulates PPR formation, we performed a microarray analysis to identify genes activated by *Zic1* in a *Xenopus* animal explant assay. Among the targets regulated by *Zic1*, we found a number of genes involved in the synthesis and metabolism of retinoic acid (RA) including lipocalin-type prostaglandin D2 synthase (*LPGDS*), retinaldehyde dehydrogenase 2 (*RALDH2*), two members of the cytochrome P450 enzyme family (*Cyp26a* and *Cyp26c*) and a cellular RA-binding protein 2 (*Crabp2*) signifying the importance of this signalling pathway in placode formation. Here we present evidence that *Zic1* regulates placode progenitor formation non-cell autonomously by controlling RA production and transport at the anterior neural plate.

Results

Identification of downstream targets of *Zic1*. The transcription factor *Zic1* is expressed at the anterior neural plate^{7–10} and is required for the formation of sensory placode progenitors⁷. To gain insights into the mechanisms by which *Zic1* regulates sensory placode formation, we performed a microarray screen to identify targets of *Zic1* (ref. 11). The screen was based on the observation that while expression of *Zic1* favoured placode fate in *Xenopus* animal cap explants, simultaneous expression of *Pax3* repressed placode-specific genes to promote neural crest fate^{7,11} (Fig. 1a). Among the genes that were both strongly upregulated by *Zic1*, as compared with *Pax3* alone, and repressed by *Pax3* co-injection, we found several well-characterized early placode-specific genes, including *Six1*, *Eya1*, *Xanf1*, *Ebf2* and *Sox11* (Fig. 1b; Supplementary Table 1). The recovery of these genes was an important validation of our experimental design. We also found several novel potential regulators of placode formation (Supplementary Table 1). These genes were initially screened by whole-mount *in situ* hybridization to select factors expressed at the anterior neural plate, in a pattern similar to *Zic1*. One candidate that fulfilled this criterion was *LPGDS* (Fig. 1c), also known as *Cpl1* (refs 12–15). By *in situ* hybridization *LPGDS* is first expressed at stage 13 in the anterior region of the neural plate (Fig. 1d). This expression pattern is maintained throughout neurulation and then appears confined to the head region in tailbud stage embryos (Fig. 1d). Double *in situ* hybridization demonstrates that *LPGDS* completely overlaps with the anterior expression domain of *Zic1* (Fig. 1e), but is excluded from the lateral expression domain of *Zic1*, which corresponds to the prospective neural crest region. *In situ* hybridization for the

neural crest-specific gene *Snail2* (ref. 16) confirmed that there is no overlap between *LPGDS* expression domain and neural crest progenitors; *LPGDS* abuts the anterior expression domain of *Snail2* (Fig. 1e).

To further establish that *LPGDS* is a true target of *Zic1*, we analysed *LPGDS* expression pattern in embryos injected with *Zic1GR* messenger RNA (mRNA) (a hormone-inducible version of *Zic1* fused to human glucocorticoid receptor (GR) ligand-binding domain), or a morpholino antisense oligonucleotide that blocks *Zic1* function (*Zic1-MO*)^{7,9}. In embryos injected with *Zic1GR* mRNA and treated with dexamethasone, we observed a marked upregulation and expansion of the *LPGDS* expression domain (Fig. 1f,g). The same injection in the absence of dexamethasone had no effect on *LPGDS* expression (Fig. 1f,g). Conversely, injection of *Zic1-MO* completely inhibited *LPGDS* expression on the injected side (Fig. 1h,i). Interestingly, in both situations we observed a reduction of *Foxi1c* and *Six1* expression, two early PPR-specific genes (Fig. 1f–i). These observations confirm that *LPGDS* is a downstream target of *Zic1* and indicate that placode formation is sensitive to *Zic1* and *LPGDS* expression levels in the embryos.

***LPGDS* is required for placode formation.** The expression pattern of *LPGDS* at the anterior neural plate and its regulation by *Zic1* suggest a potential role in placode formation. To test this possibility, we used a translation-blocking morpholino antisense oligonucleotide (*LPGDS-MO*) to interfere with *LPGDS* function. The activity of the morpholino was confirmed in an *in vitro* transcription/translation assay in which *LPGDS-MO* blocked *LPGDS* protein production (Fig. 2a; Supplementary Fig. 1). Unilateral injection of *LPGDS-MO* (40 ng) in the animal pole region of two-cell stage embryos resulted in a marked decrease expression of *Six1* (refs 17,18), *Foxi1c*^{18,19} and *Sox2* (ref. 20), three genes broadly expressed at the PPR (Fig. 2b,d). We also analysed the expression of genes restricted to individual placodal domains such as *Dmrt4* for the adenohipophyseal and olfactory placodes²¹, *Pax8* for the otic and lateral line placodes²² and *Tbx2* for otic and trigeminal/profundal placodes²³. For each one of these genes a significant reduction of expression was observed on the injected side (Fig. 2c) in >80% of the embryos (Fig. 2d). Injection of a control morpholino (Cont-MO) had no effect on the expression of these genes (Supplementary Fig. 2e). To further establish the specificity of *LPGDS* knockdown phenotype, we used a second morpholino (*LPGDS-MO2*) that specifically interfered with *LPGDS* pre-mRNA splicing by targeting intron 1/exon 2 junction (Supplementary Fig. 2a), resulting in the production of a transcript of higher size, due to intron retention (Supplementary Fig. 2b). The phenotype of *LPGDS-MO2*-injected embryos was indistinguishable from the phenotype generated by injection of the translation-blocking morpholino, with inhibition of *Foxi1c*, *Six1* and *Dmrt4*, although at a lower frequency (Supplementary Fig. 2c,d). These results indicate that *LPGDS* is critically required for the establishment of the PPR and for sensory placode formation.

LPGDS functions independently of its enzymatic activity.

LPGDS has a dual function, as an enzyme involved in the biosynthesis of prostaglandin D2 (PGD2) from its precursor, and as a lipophilic ligand-binding protein when secreted²⁴. The *LPGDS* molecule contains three cysteine residues, and site-directed mutagenesis has established that the cysteine residue at position 65 (Cyst65) is essential for the enzymatic activity of *LPGDS*²⁵, a cysteine highly conserved from human to frogs (Fig. 2e). To determine whether *LPGDS* regulates placode formation through PGD2 signalling, we performed a rescue experiment using mRNA

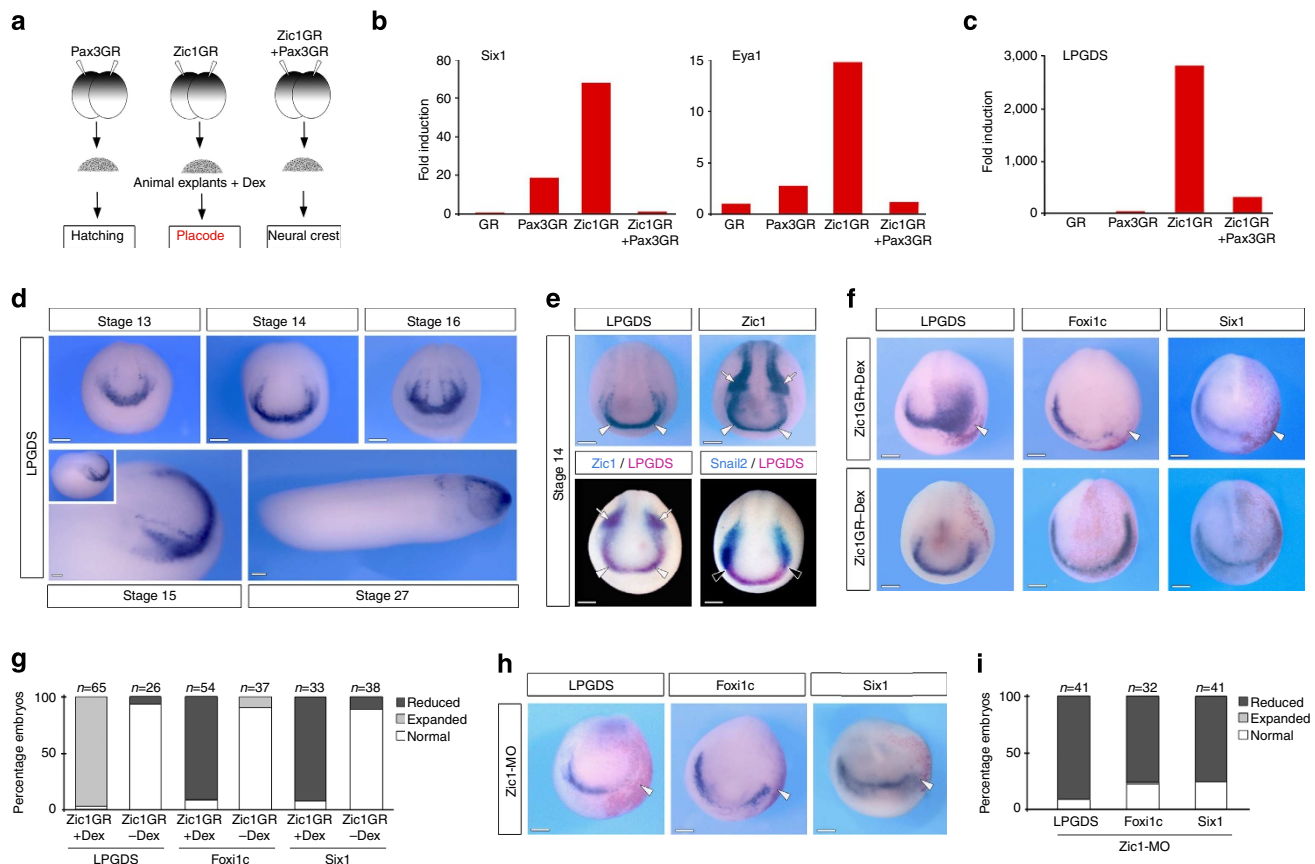


Figure 1 | LPGDS is a downstream target of Zic1. (a) Experimental design for the selection of Zic1 targets. (b) Fold induction of *Six1*, *Eya1* and (c) *LPGDS* from the microarray data. (d) *In situ* hybridization for *LPGDS* (stages 13, 14 and 16 are frontal views; stage 15 and stage 27 are lateral views, anterior to right, dorsal to top). (e) *In situ* hybridization for *LPGDS* and *Zic1* in stage-matched embryos (upper panels). *LPGDS* and *Zic1* co-localize at the anterior neural plate (arrowheads), while *Zic1* is also expressed in neural crest progenitors (arrows). Double *in situ* hybridization (lower panels) shows overlapping expression of *LPGDS* and *Zic1* at the anterior neural plate (arrowheads; left panel), while *LPGDS* and *Snail2* (right panel) have adjacent but non-overlapping expression domains (black arrowheads). Frontal views. (f) In embryos injected with *Zic1GR* mRNA and treated with dexamethasone (+ Dex), *LPGDS* is markedly expanded (arrowhead), while *Foxi1c* and *Six1* expression at the PPR are reduced (arrowheads). The same injection in the absence of dexamethasone (- Dex) had no effect on the expression of these genes. Frontal views, the injected side is indicated by the lineage tracer (Red-Gal). (g) Quantification of the *Zic1GR* injection results. Three independent experiments were performed. The number of embryos analysed (*n*) is indicated on the top of each bar. (h) *Zic1* knockdown (*Zic1*-MO injection) reduces *LPGDS*, *Foxi1c* and *Six1* expression. (i) Quantification of the *Zic1*-MO injection results. Three independent experiments were performed. The number of embryos analysed (*n*) is indicated on the top of each bar. Scale bars, 200 µm.

encoding wild-type (WT) mouse *LPGDS* or a mutated version in which Cyst65 has been replaced by an alanine (C65A), thereby completely abolishing the enzymatic activity of *LPGDS*²⁵. Embryos at the two-cell stage were sequentially injected with *LPGDS*-MO and either with WT or C65A mouse *LPGDS* mRNA. Both mRNA were equally efficient at rescuing *Foxi1c* and *Six1* expression in morphant embryos (Fig. 2f,g). Complementary to this rescue assay, we found that well-characterized pharmacological agents that specifically block the PGD2 signalling pathway did not affect *Foxi1c* expression at the PPR (Supplementary Fig. 3). Altogether, these results demonstrate that *LPGDS* regulates placode formation through a mechanism that does not involve its enzymatic activity and the production of PGD2.

LPGDS functions as a carrier for RA. Since *LPGDS* binds retinoids with high affinity^{14,26}, we wished to determine whether *LPGDS* regulated placode formation through this mechanism. As a preliminary evaluation, we treated intact embryos at the gastrula stage (stage 11) with increasing doses of RA (0.01–10 µM) and analysed the consequence on PPR formation. We found that the lower doses of RA (0.01 and 0.1 µM) resulted

in an expansion of *Foxi1c* and *Six1* expression domains, while the higher doses of RA (1 and 10 µM) inhibited the expression of both genes (Fig. 3), indicating that PPR formation is very sensitive to RA levels in the embryo. On the basis of these observations, we performed a rescue experiment in which *LPGDS*-MO-injected embryos were exposed at stage 11 to 0.1 µM of RA (the dose of RA that promotes strong expansion of PPR genes; Fig. 3) or a RA receptor (RAR) agonist, TTNPB²⁷. Both treatments efficiently rescued *Foxi1c* and *Six1* expression in morphant embryos and occasionally expanded *Foxi1c* and *Six1* expression on the control side (Fig. 4a,b). *LPGDS* can also bind retinaldehyde (retinal), the RA precursor, with high affinity^{14,26}; however, this compound was unable to rescue the *Foxi1c* expression domain in *LPGDS*-depleted embryos (Supplementary Fig. 4), indicating that in the context of PPR formation *LPGDS* is functioning primarily as a RA carrier, and that RA is the active compound promoting PPR formation.

Zic1 regulates *RALDH2* expression. Our results suggest that *LPGDS* activity at the anterior neural plate is linked to RA activity. Consistent with this observation, we found several

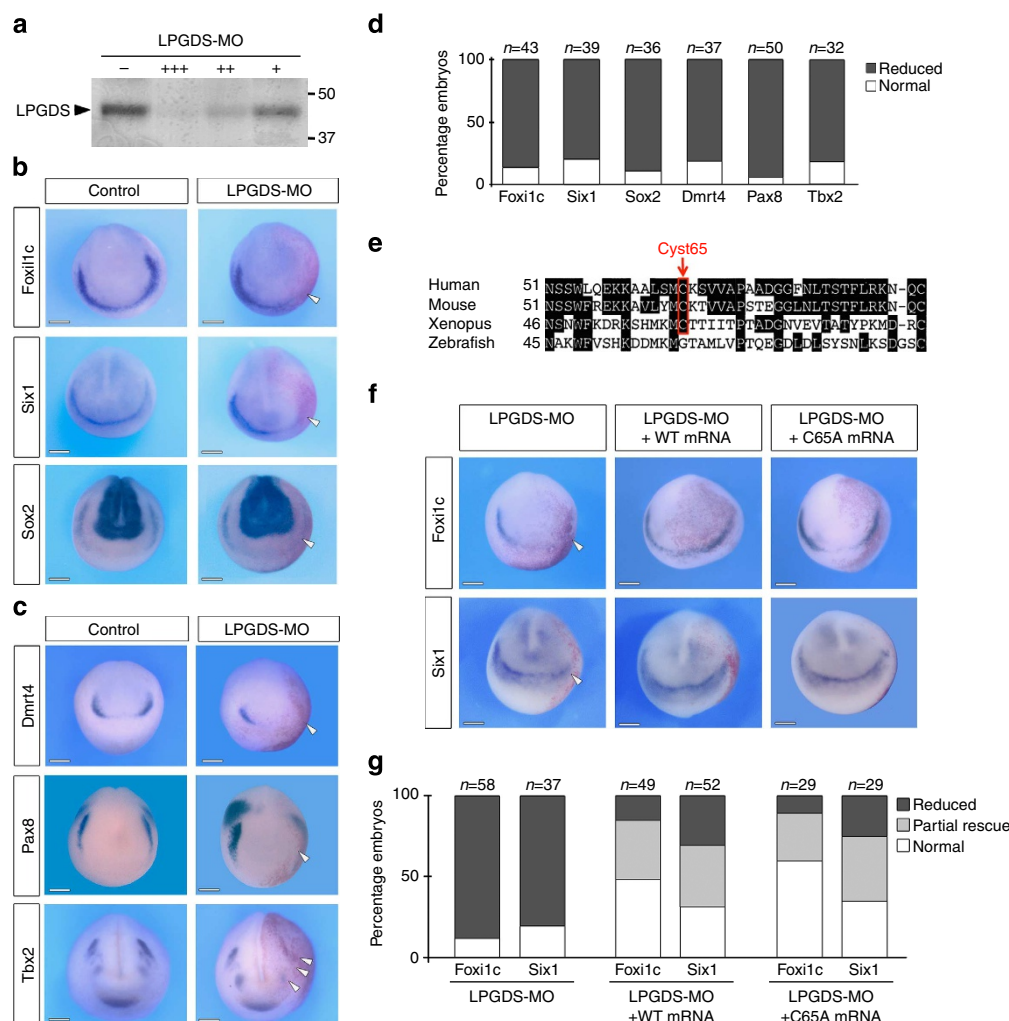


Figure 2 | LPGDS is required for placode development. (a) Increasing amounts of LPGDS-MO 10 ng (+), 100 ng (++) and 1,000 ng (+++) blocks translation directed by *LPGDS* mRNA in an *in vitro* coupled transcription/translation reaction. The position of markers of known molecular weight (kDa) is indicated. (b) *In situ* hybridization for pan-placodal and (c) placode-specific genes in control and LPGDS-MO-injected embryos (frontal views, dorsal to top). Arrowheads indicate reduced expression on the injected side. (d) Quantification of the results. Four independent experiments were performed. The number of embryos analysed (*n*) is indicated on the top of each bar. (e) Amino-acid sequence alignment showing the conserved cysteine residue (Cyst65), centre of *LPGDS* enzymatic activity. (f) *Foxi1c* and *Six1* expression domains are rescued in LPGDS-MO-injected embryos by co-injection of either WT or C65A mouse *LPGDS* mRNA. Frontal views, dorsal to top; injected side is indicated by the lineage tracer (Red-Gal). (g) Quantification of the rescue experiment. Three independent experiments were performed. The number of embryos analysed (*n*) is indicated on the top of each bar. LPGDS-MO vs LPGDS-MO + WT or LPGDS-MO + C65A mRNA-injected embryos ($P < 0.001$, Fisher's exact test.); LPGDS-MO + WT mRNA vs LPGDS-MO + C65A mRNA-injected embryos show no significant differences. Scale bars, 200 μ m.

components of RA metabolism and function strongly upregulated by *Zic1* in the microarray screen (Supplementary Table 1). These include *RALDH2*, the enzyme responsible for the synthesis of RA from its precursor retinal, two RA-degrading enzymes (*Cyp26a* and *Cyp26c*) and a cellular RA-binding protein 2 (*Crabp2*). In the microarray samples, *RALDH2* induction levels followed the same pattern as *LPDGS* (Fig. 4c). *RALDH2* is expressed in the trunk mesoderm, as well as in a discrete U-shaped ectodermal domain around the anterior neural plate, similar to *LPGDS* (Fig. 4d)²⁸. *Zic1* knockdown reduced *RALDH2* expression in the embryo (Fig. 4e), confirming that *RALDH2* is functioning downstream of *Zic1*. Moreover, in the absence of *RALDH2* function, *Foxi1c* was severely reduced at the PPR (Fig. 4f), further demonstrating the link between *Zic1*, *RALDH2* activity and placode formation.

***Zic1* induces placode fate non-cell autonomously.** Our data indicate that *Zic1* may control RA signalling at the anterior neural

plate through the activation of *RALDH2* to produce RA and *LPGDS* to transport RA extracellularly. *Zic1*, *RALDH2* and *LPGDS* are all confined to the anterior neural plate, at a distance from the prospective PPR (*Foxi1c*-expressing cells; Fig. 5a), suggesting that *Zic1* regulates placode formation non-cell autonomously. To test this possibility, embryos were injected in one blastomere at the two-cell stage with *Zic1GR* mRNA and mRNA encoding the lineage tracer green fluorescent protein (GFP), animal explants isolated at the blastula stage, treated with dexamethasone and cultured for 8 h (Fig. 5b). Injection of GR mRNA was used as a negative control (Supplementary Fig. 5). Explants were then processed for *in situ* hybridization on sections. In these explants, *Six1* and *Foxi1c* expression was exclusively confined to GFP-negative cells, derived from the uninjected blastomere (Fig. 5c; upper panels). By contrast, *LPGDS* and *RALDH2* expression was always closely associated with *Zic1GR*/GFP-positive cells (Fig. 5c; lower panels). Altogether, these results demonstrate that *Zic1* is

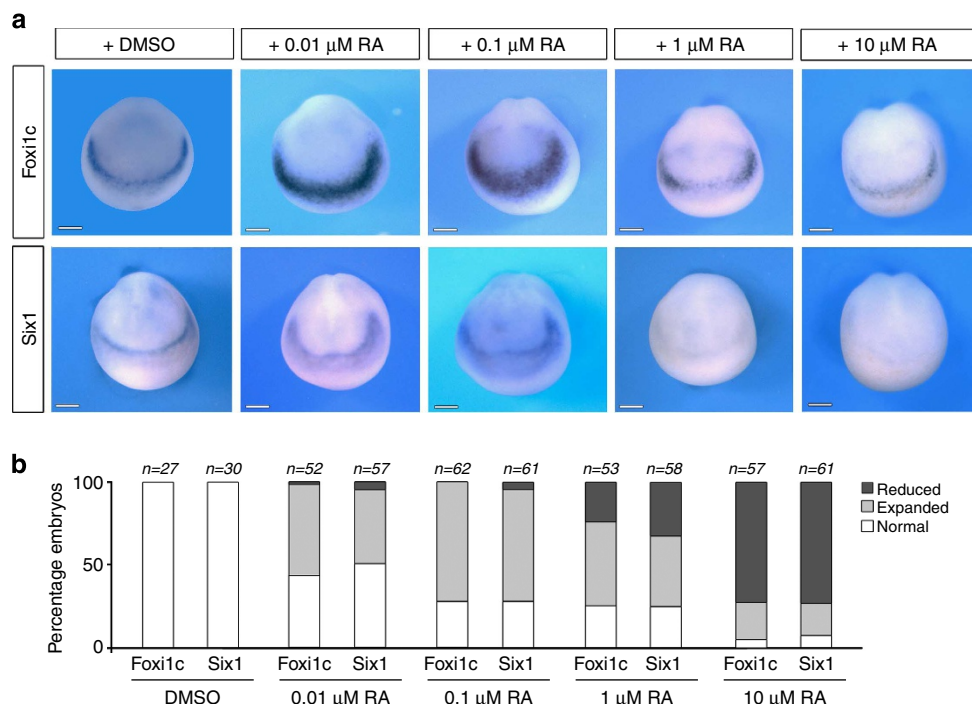


Figure 3 | Retinoic acid affects PPR formation in a dose-dependent manner. (a) Treatment of intact embryos at stage 11 with increasing doses of RA (0.01, 0.1, 1 and 10 μM) disrupts *Foxi1c* and *Six1* expression at the PPR. Dimethylsulphoxide (DMSO) was used as a control. Frontal views, dorsal to top. (b) Quantification of the results. Four independent experiments were performed. The number of embryos analysed for each condition (n) is indicated on the top of each bar. Scale bars, 200 μm.

inducing placode fate by a non-cell autonomous mechanism involving activation of RA signalling.

Zic1-activated RA signalling uses non-canonical RARs. To further establish that the placode-inducing activity of Zic1 depends on active RA signalling, we analysed by reverse transcription (RT)-PCR the expression of *Six1* and *Eya1* in Zic1GR-injected animal explants treated with 100 μM of disulfiram or citral (Fig. 6a), two general inhibitors of alcohol and aldehyde dehydrogenases^{29,30}, the group of enzymes that sequentially catalyse the oxidation of retinol and retinaldehyde to produce RA. In these animal explants treated with the inhibitors, the induction of *Six1* and *Eya1* by Zic1GR was significantly reduced (Fig. 6b; Supplementary Fig. 6a,b), consistent with the view that placode induction by Zic1 depends on RA production.

To determine whether the placode-inducing activity of Zic1 is mediated through canonical RARs, Zic1GR-injected animal explants were treated with a well-characterized pan-RAR antagonist, AGN193109 (refs 31,32) (Fig. 6a). Surprisingly, we found that AGN193109 was unable to block the expression of *Six1* and *Eya1* (Fig. 6c; Supplementary Fig. 6c), while the same concentration of antagonist (10 μM) was extremely efficient at repressing *Hnf1b* expression in the whole embryo (Fig. 6d), a gene directly regulated by RAR signalling³³. These results suggest that Zic1-activated RA signalling mediates its activity through a mechanism that does not involve canonical RARs, and may signal through other nuclear receptors that also bind RA, such as peroxisome proliferator-activated receptor β (ref. 34), and members of the RAR-related orphan receptors^{35,36}.

Discussion

Our findings uncover the non-cell autonomous activity of Zic1 in the control of placode fate, and implicate RA signalling as a major

player in cranial placode progenitor formation. We have identified several genes activated by Zic1 that are involved in RA metabolism and function. Among them we demonstrate that *RALDH2* and *LPGDS*, respectively, are responsible for the synthesis and the transport of RA, and directly participate in the establishment of the PPR. We propose that the activation of *RALDH2* and *LPGDS* at the anterior neural plate by Zic1 allows for the localized production and transport of RA, which in turn activates a placode developmental programme in neighbouring cells (Fig. 7).

Xenopus LPGDS, also known as *cpl1* (choroid plexus lipocalin 1), was first isolated in a screen for genes activated at gastrulation and specifically expressed in the nervous system¹⁵, and has been primarily used as a forebrain marker^{12,13,37}. Its specific role at the anterior neural plate has not been studied. *Cpl1/LPGDS* was also isolated in another screen designed to identify direct targets of Zic1 (ref. 38); however, further studies are needed to confirm that Zic1 directly activates *LPGDS* expression. *LPGDS* is a bifunctional protein that acts as a PGD2-producing enzyme and a lipophilic ligand-binding protein³⁹. More specifically, *LPGDS* can bind retinaldehyde and RA with high affinities^{13,14,26}. In a rescue assay, using WT and mutant versions of mouse *LPGDS* we completely ruled out the involvement of its enzymatic activity, and demonstrated that *LPGDS* functions during placode formation through a mechanism implicating RA signalling. By exposing the entire embryo to RA, the expression of PPR genes was efficiently rescued in *LPGDS*-depleted embryos (Fig. 4a,b). In these experiments, the exogenous source of RA bypasses the requirement for an *LPGDS*-mediated transport of RA to the PPR. We posit that *LPGDS* is essential to transport RA outside the producing cells. *LPGDS* knockdown in the embryo leads to a loss of genes expressed at the PPR, as well as genes that are more specific for individual cranial placodes, suggesting a broad requirement for *LPGDS* and RA signalling in placode progenitor formation.

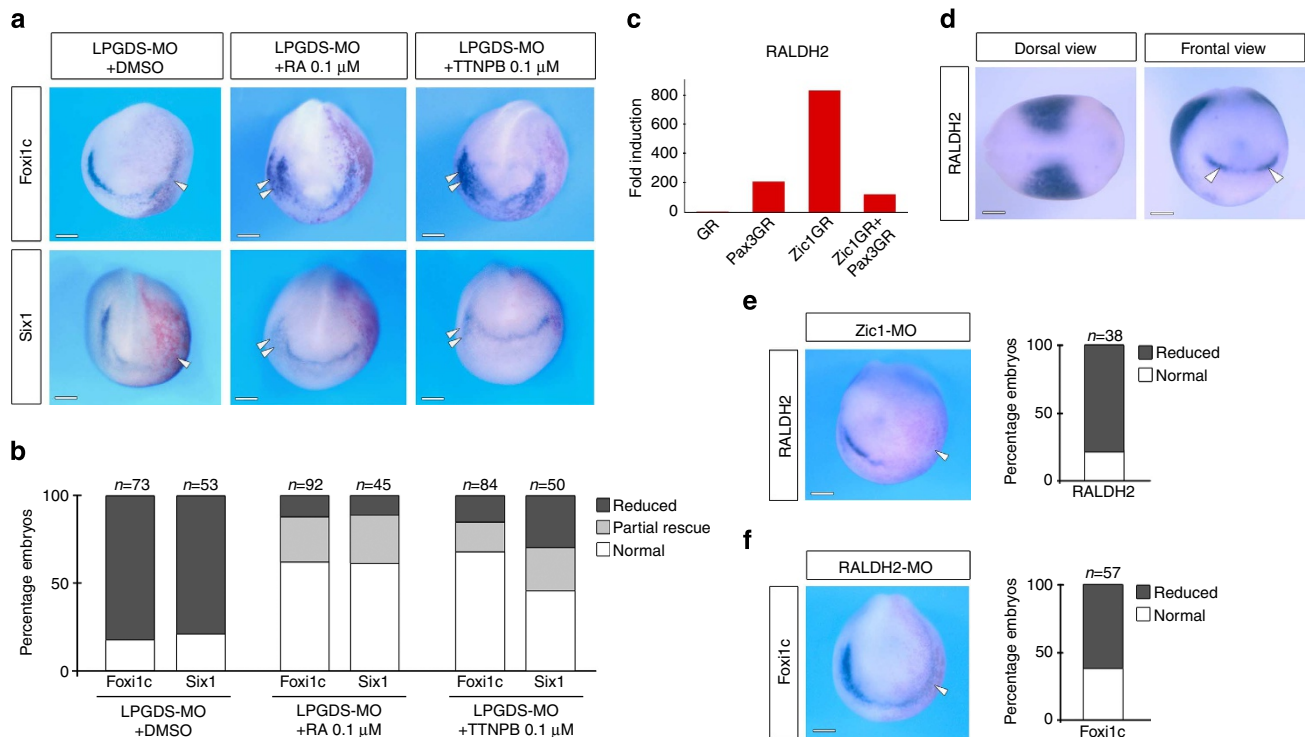


Figure 4 | Retinoic acid signalling regulates placode formation. (a) Treatment at stage 11 of LPGDS-depleted embryos (LPGDS-MO) with 0.1 μ M RA or with the RA receptor agonist, TTNPB, restored completely or partially *Foxi1c* and *Six1* expression on the injected side. Frontal views, dorsal to top. Injected side is indicated by the lineage tracer (Red-Gal). Double arrowheads indicate *Foxi1c* or *Six1* expansion on the control side. (b) Quantification of the rescue experiment. Four independent experiments were performed. The number of embryos analysed for each condition (*n*) is indicated on the top of each bar. Dimethylsulphoxide (DMSO) vs RA- or TTNPB-treated embryos ($P < 0.001$, Fisher's exact test) RA- vs TTNPB-treated embryos show no significant differences. (c) Fold induction of *RALDH2* from the microarray data. (d) By *in situ* hybridization *RALDH2* is detected in the trunk mesoderm (dorsal view, anterior to right) and at the anterior neural plate (frontal view; arrowheads). (e) *RALDH2* expression is lost in *Zic1*-depleted embryos. The graph is a quantification of the results. Three independent experiments were performed. The number of embryos analysed (*n*) is indicated on the top of the bar. (f) *Foxi1c* expression is reduced in *RALDH2*-MO-injected embryos. The graph is a quantification of the results. Three independent experiments were performed. The number of embryos analysed (*n*) is indicated on the top of the bar. (e,f) Arrowheads indicate reduced expression on the injected side. Scale bars, 200 μ m.

A recent study has proposed that signalling through RARs (*RAR α 2*), which are expressed in the caudal half of the embryo⁴⁰, was critical to set up the posterior boundary of the PPR⁴¹. Our experiments using the pan-RAR antagonist (AGN193109) suggest that the placode-inducing activity of *Zic1* may use an RAR-independent pathway, pointing to the intriguing possibility that another set of receptors may mediate this activity. A similar activity of RA, independent of canonical RARs, has been described in the context of the developing mouse neural retina⁴². Several classes of nuclear receptors have been reported to bind RA, including peroxisome proliferator-activated receptor β (ref. 34) and members of the RAR-related orphan receptors^{35,36}, and are therefore potential candidates to mediate the placode-inducing activity of *Zic1*. Future work will test this hypothesis.

During embryonic development, RA signalling is essential for the regionalization of the embryo along the anteroposterior axis. Studies in several organisms have shown that RA is an important posteriorizing signal in all three germ layers, acting in concert with molecules of the Wnt and FGF families^{43–45}. However, RA signalling may have a more direct role in PPR specification, independent of its posteriorizing activity, in a similar manner as the posteriorizing activity of FGF, and canonical Wnt can be uncoupled from their role in neural crest induction^{10,46}. Consistent with this possibility, *RALDH2* has two major expression domains in the early embryo: the paraxial and lateral plate mesoderm in the trunk region, as well as a discrete

U-shaped ectodermal domain around the anterior neural plate²⁸ (Fig. 4d). While the former has been linked to the posteriorizing activity of RA, the latter represents an independent source of RA, and we propose that this anterior domain is essential to pattern the cranial region of the embryo. In a recent study using novel transgenic RA sensor lines, RA activity has been visualized at the very anterior region of the zebrafish embryo and at the polster, and a candidate source of this activity is *RALDH3* (ref. 47). In the mouse, *RALDH2* is responsible for RA signalling in the early embryonic head, and knockout embryos die around E9.5–10.5 with severe forebrain and craniofacial defects⁴⁸. In birds, *RALDH3* is expressed anteriorly at early stages⁴⁹, and vitamin A-deficient quail embryos have defective otic vesicles and lack the pituitary gland, two derivatives of cranial placodes^{50,51}.

Zic1 gain of function resulted in a marked upregulation of *LPGDS* in the embryo, which was surprisingly associated with a loss of early placode markers (*Six1* and *Foxi1c*; Fig. 1f). However, in light of our results linking *Zic1* to RA signalling, this result is not completely unexpected and indicates that PPR formation is very sensitive to RA levels. As in other RA-regulated developmental processes, excess or insufficient RA signalling often result in similar outcomes⁴⁵. Excess RA can shut down its own production through the downregulation of *RALDH2* (ref. 52). Indeed, in embryos treated with RA, *RALDH2* is preferentially lost anteriorly, leading to severe head truncation²⁸. Furthermore, exposure of intact embryos to varying doses of RA affects PPR

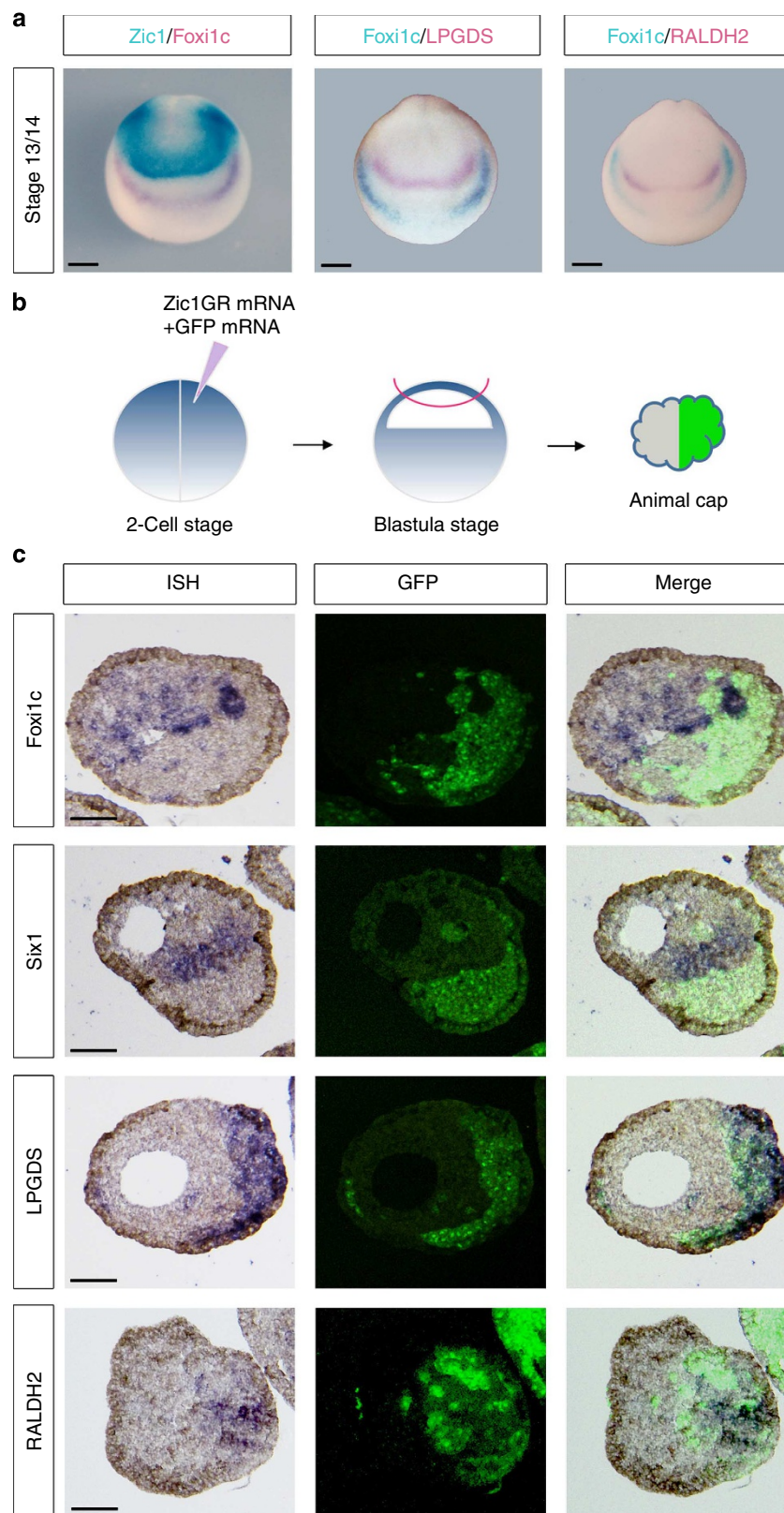


Figure 5 | Zic1 regulates placode formation non-cell autonomously. (a) Double *in situ* hybridization for *Zic1*/*Foxi1c*, *Foxi1c*/LPGDS and *Foxi1c*/RALDH2 showing that *Zic1*, LPGDS and RALDH2 are expressed at a distance from the PPR (*Foxi1c*-expressing cells). Frontal views, dorsal to top. Scale bars, 200 μ m. (b) Animal explants dissected from embryos injected in one blastomere at the two-cell stage with Zic1GR and GFP mRNAs were cultured for 8 h in dexamethasone and analysed by *in situ* hybridization (ISH). (c) ISH for *Foxi1c*, *Six1*, LPGDS and RALDH2 on sections of animal explants derived from embryos injected with Zic1GR and GFP mRNA in one blastomere at the two-cell stage (left panels). In each case the Zic1GR-expressing cells (GFP positive) are shown (middle panels). Merge of fluorescence and ISH images (right panels). Three independent experiments were performed with similar results for each probe as pictured (*Foxi1c*, $n = 14$; *Six1*, $n = 13$; LPGDS, $n = 13$ and RALDH2, $n = 11$). Scale bars, 100 μ m.

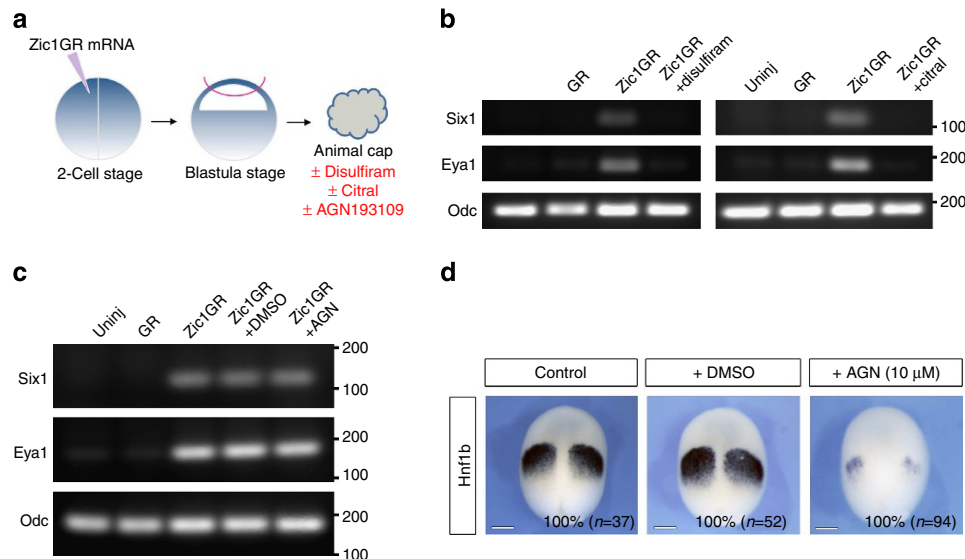


Figure 6 | Zic1 regulates placode fate independently of canonical RA receptors. (a) Animal explants dissected from embryos injected in one blastomere at the two-cell stage with Zic1GR mRNA and cultured for 8 h in dexamethasone, with or without the pharmacological inhibitors disulfiram (100 μ M), citral (100 μ M) or AGN193109 (10 μ M). (b) RT-PCR analysis of *Six1* and *Eya1* expression in animal explants expressing Zic1GR treated with disulfiram or citral. *Odc* (ornithine decarboxylase) is shown as a loading control. Controls are uninjected (Uninj) and GR mRNA-injected (GR) animal explants. Similar results were obtained in four independent experiments for each inhibitor. The position of markers of known size is indicated (bp). (c) RT-PCR analysis of *Six1* and *Eya1* expression in Zic1GR-injected animal explants treated with the pan-RAR antagonist, AGN193109. Controls are uninjected (Uninj), GR mRNA-injected (GR) and Zic1GR mRNA-injected treated with dimethylsulphoxide (+ DMSO) animal explants. Similar results were obtained in six independent experiments. The position of markers of known size is indicated (bp). (d) AGN193109 treatment blocks *Hnf1b* expression in the posterior hindbrain (100% of the embryos; $n = 94$), while in DMSO-treated embryos *Hnf1b* expression is similar to that of control embryos (100% of the embryos; $n = 52$ and $n = 37$, respectively). Three independent experiments were performed. Stage 13 embryos, dorsal views, anterior to top. Scale bars, 200 μ m.

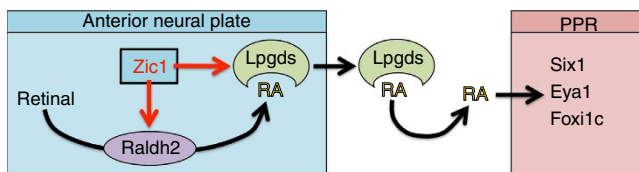


Figure 7 | Model for the regulation of PPR formation by Zic1 and RA signalling. Zic1 controls RA signalling at the anterior neural plate through the activation of RALDH2 to produce RA, and LPGDS to transport RA extracellularly. As a consequence, RA induces the expression of *Six1*, *Eya1* and *Foxi1c* in neighbouring cells (PPR).

gene expression in a concentration-dependent manner (Fig. 3). Altogether, these observations support the view that RA levels at the anterior neural plate are critical for placode formation.

The non-cell autonomous activity of Zic1 in the control of placode fate was especially evident in the animal explant system (Fig. 5). Interestingly, we never observed the activation of *Six1* or *Foxi1c* in Zic1GR-expressing cells, rather the expression of *Six1* and *Foxi1c* was always confined to adjacent cells, derived from the uninjected blastomere. A possible explanation is related to the activity of Cyp26c and Cyp26a, the RA-metabolizing enzymes, which were strongly upregulated by Zic1GR in the microarray. Typically, RA is released by RA-producing cells and can enter adjacent cells where it faces two scenarios: (i) in cells expressing Cyp26, RA is degraded preventing RA signalling and (ii) in cells that do not express Cyp26, RA enters the nucleus and initiates the transcription of target genes. It is possible that Cyp26 expression renders Zic1-expressing cells refractory to RA signalling, thereby allowing for the unidirectional propagation of the RA signal, and the establishment of sharp boundaries of gene expression.

Consistent with this interpretation, in *Xenopus* *Cyp26c* is expressed in the neural plate but is excluded from the most anterior region of the embryo⁵³.

While the placode-inducing activity of Zic1 requires active RA signalling, RA is likely to act in concert with other signals to impart placode fate. Work in zebrafish suggests that Zic1 is functioning not only upstream of RA, but also by regulating Nodal and Hedgehog signalling to control midline tissue development in the head^{54,55}. These factors are therefore good candidates to synergize with RA to promote cranial placode fate.

Methods

Plasmids, constructs and oligonucleotides. *Xenopus laevis* Pax3GR and Zic1GR, the hormone-inducible versions of Pax3 and Zic1, fused to the human glucocorticoid receptor (GR) ligand-binding domain⁵⁶, wild type (WT) and mutated (C65A) mouse *LPGDS* (refs 7,25) were subcloned into pCS2+ expression plasmid. Pax3GR, Zic1GR, GR, WT and C65A mouse *LPGDS*, GFP and β -galactosidase mRNAs were synthesized *in vitro* using the Message Machine Kit (Ambion, Austin, TX). Zic1 (Zic1-MO)⁹, RALDH2 (RALDH2-MO)²⁹ and LPGDS (LPGDS-MO: 5'-TCAGAGCAAGCAAATCCTCATCAT-3'; LPGDS-MO2: 5'-AGACCTAG AGGCAGAGAGAGGAATT-3') morpholino antisense oligonucleotides were purchased from GeneTools (Philomath, OR). The specificity of the LPGDS-MO was tested in an *in vitro* transcription/translation-coupled rabbit reticulocyte lysate assay (Promega, Madison, WI). LPGDS-MO was designed to interfere with both LPGDS-a and LPGDS-b function (accession numbers: NM_001092825 and NM_001088044), while LPGDS-MO2 interfered only with LPGDS-a. A standard morpholino (Cont-MO; 5'-CCTCTTACCTCAGTTACAATTATA-3') was used as control.

Embryos, injections and explant culture. *X. laevis* embryos were staged according to Nieuwkoop and Faber⁵⁷ and raised in 0.1 \times NAM (normal amphibian medium)⁵⁸. This study was performed in accordance with the recommendations of the Guide for the Care and Use of Laboratory Animals of the National Institutes of Health. The procedures were approved by the Institutional Animal Care and Use Committee of New York University under animal protocol #120311. Embryos were injected in one blastomere at the two-cell stage and analysed by *in situ* hybridization at stage 15. Morpholino antisense

oligonucleotides (40–50 ng) were injected together with 0.5 ng of β -galactosidase mRNA as a lineage tracer. Rescue experiments were performed by sequential injection of LPGDS-MO and 0.5 ng of WT or C65A mouse *LPGDS* mRNA. For all-trans RA and TTNPB (Sigma-Aldrich, St. Louis, MO) treatments, control and LPGDS-MO-injected embryos were incubated at stage 11 in the retinoids (0.01, 0.1, 1 and 10 μ M diluted in 0.1 \times NAM) and collected at stage 15 for *in situ* hybridization. Control and LPGDS-MO-injected embryos treated with dimethylsulphoxide were used as control. For animal explant experiments, one blastomere at the two-cell stage was injected in the animal pole region with *GR* or *Zic1GR* mRNA (0.5–1 ng), explants were dissected at the late blastula stage and immediately cultured for several hours in NAM 0.5 \times plus 10 μ M of dexamethasone (Sigma-Aldrich). Co-injection of 1 ng of *GFP* mRNA was used as a lineage tracer to identify the progeny of the injected blastomere. Dissected animal explants injected with *Zic1GR* mRNA were treated with 100 μ M disulfiram (tetraethylthiuram disulfide) or citral (Sigma-Aldrich), two general inhibitors of alcohol and aldehyde dehydrogenases, or with 10 μ M of AGN193109 (Santa Cruz Biotechnology, Dallas, TX), an RAR antagonist.

In situ hybridization. Embryos were fixed in MEMFA (0.1 M 3-(N-Morpholino)-propanesulfonic acid, pH 7.4, 2 mM EGTA, 1 mM MgSO₄ and 3.7% formaldehyde) and prior to *in situ* hybridization the β -galactosidase activity was revealed using Red-Gal (Research Organics, Cleveland, OH). Whole-mount *in situ* hybridization³⁹ was performed in 4-ml glass vials using digoxigenin (DIG)- and fluorescein isothiocyanate (FITC)-labelled antisense RNA probes (Genius Kit; Roche, Indianapolis, IN) synthesized from template complementary DNA (cDNA) encoding *Zic1* (ref. 20), *Foxi1c*^{18,19}, *Six1* (ref. 17), *Sox2* (ref. 20), *Dmrt4* (ref. 21), *Pax8* (ref. 22), *Tbx2* (ref. 23), *LPGDS* (pSPORT6-LPGDS; Open Biosystems), *RALDH2* (ref. 29) and *Snail2* (ref. 16). Embryos were hybridized overnight at 60 °C. RNA probes were detected using an anti-DIG antibody conjugated to alkaline phosphatase (Roche) at a 1:2,000 dilution overnight at 4 °C. After several washes, the chromogenic reaction was performed overnight by incubation in BM purple (Roche). The reaction was then stopped by fixation in MEMFA and the embryos were bleached in 10% hydrogen peroxide in methanol for 48 h. For double *in situ* hybridization, DIG- and FITC-labelled probes were hybridized simultaneously and sequentially detected using anti-FITC- and anti-DIG alkaline phosphatase-conjugated antibodies (Roche; 1:10,000 and 1:2,000 dilution, respectively). FITC-labelled probe was visualized first using Magenta Phosphate (5-bromo-6-chloro-3-indoxyl phosphate; Biosynth, Itasca, IL) and after inactivation of the anti-FITC antibody by treatment with glycine (0.1 M, pH 2.2) for 30 min, the colour reaction for the DIG-labelled probe was performed using 4-toluidine salt (BCIP; Roche). The reaction was then stopped by fixation in MEMFA and the embryos were bleached in 10% hydrogen peroxide in PBS for 48 h. For *in situ* hybridization on sections, animal explants were fixed in 4% paraformaldehyde in PBS (Gibco, Grand Island, NY) for 1 h, embedded in Paraplast+ and 12- μ m sections were collected on a glass slide and hybridized overnight at 60 °C in a humidified chamber with *Foxi1c*, *Six1*, *LPGDS* or *RALDH2* DIG-labelled probes. Sections were then washed in 2 \times saline sodium phosphate EDTA (Invitrogen, Grand Island, NY). Probes were detected using an anti-DIG antibody conjugated to alkaline phosphatase at a 1:2,000 dilution for 2 h at room temperature. After several washes, the chromogenic reaction was performed overnight by incubation in BM purple (Roche). The reaction was stopped by fixation in MEMFA. The slides were then dehydrated and mounted in Permount (Fisher Scientific, Pittsburgh, PA)⁶⁰. Since GFP can no longer be detected following this procedure, sections of GFP-labelled animal explants were first individually photographed and then processed for *in situ* hybridization.

RT-PCR analysis. Total RNAs were extracted from 10–15 animal explants using the RNeasy microRNA isolation kit (Qiagen, Valencia, CA). To avoid contamination from genomic DNA, the RNA samples were digested with RNase-free DNase I. RT-PCR experiments were performed using the One Step RT-PCR kit (Qiagen) according to the manufacturer's instructions using the following primer sets: *Six1* (F: 5'-CTGGAGAGCCACAGTTCTC-3'; R: 5'-AGTGGTCTCCCC TCAGTTT-3'; 30 cycles), *Eya1* (F: 5'-ATGACACCAATGGCAGACA-3'; R: 5'-GGGAAACTGGTGTGCTGTG-3'; 30 cycles) and *Odc* (F: 5'-ACATGGCA TTCTCCCTGAAG-3'; R: 5'-TGGTCCCAAGGCTAAAGTTG-3'; 25 cycles).

Microarray analysis. RNAs were extracted from animal explants expressing *GR*, *Pax3GR*, *Zic1GR* or a combination of *Pax3GR* and *Zic1GR* using the RNeasy microRNA isolation kit. During the extraction procedure, the samples were treated with DNase I to eliminate possible genomic DNA contamination. The amount of isolated RNA was quantified using a spectrophotometer. Extracted RNAs (five replicate for each injection set) were used for the microarray experiment. Probe labelling, hybridization and initial data analysis were performed at the University of Pennsylvania Microarray Facility. Around 0.1–0.2 μ g total RNA was converted into first-strand cDNA using Superscript II reverse transcriptase primed by a poly(T) oligomer that incorporates the T7 promoter. Second-strand cDNA synthesis is followed by *in vitro* transcription for linear amplification of each transcript and incorporation of biotinylated nucleotides. The cRNA products were fragmented to 200 nucleotides or less, heated at 99 °C for 5 min and hybridized for 16 h at 45 °C to

a GeneChip *Xenopus laevis* Genome 2.0 Array (Affymetrix, Cleveland, OH). Hybridized arrays were processed by the GeneChip Fluidics system, and scanned in the GeneChip Scanner. Probe intensities were exported in cel files using GCOS software (Affymetrix). Subsequent quantification of expression levels and statistical identification of differentially regulated genes was performed using Partek Genomics Suite (Partek, Inc., St. Louis, MO). Normalized, log₂-transformed probe intensities were calculated using GeneChip Robust Multiarray Averaging (GC-RMA). Analysis of variance with multiple testing corrections was used to determine *P* values for likelihood of differential expression, based on reproducibility in five replicates to identify cDNAs both activated by *Zic1GR* and repressed in *Zic1GR*/*Pax3GR* samples. Pairwise comparisons yielding fold changes were performed between these conditions. The microarray data have been deposited in the GEO database under the accession number GSE68546.

PGD2 signalling inhibitors and treatment. To interfere with PGD2 signalling pathway, we used well-characterized pharmacological inhibitors: AT-56 (Tocris Bioscience, Minneapolis, MN) to block LPGDS enzymatic activity, and two antagonists of PGD2 receptors, BWA868C (Cayman Chemical, Ann Arbor, MI) specific for DP1 and ramatroban (Sigma-Aldrich) specific for DP2. For treatment, embryos at stage 11 devoid of the vitelline membrane were incubated in the presence of the inhibitors (1, 10 and 100 μ M in NAM 0.1 \times), collected at stage 15 and processed for *in situ* hybridization. Dimethylsulphoxide-treated embryos were used as control.

Imaging. Images were captured using an Olympus SZX9 microscope and a QImaging Micro Publisher 3.3 RTV camera. Images from sections of animal explants were obtained on a Nikon SMZ1500 microscope equipped with a Nikon Ds-U3 camera. Composite images were assembled using Adobe Photoshop. In some experiments RFP mRNA was injected as a lineage tracer, in place of GFP mRNA and for consistency, the images were then digitally coloured (green) using ImageJ; this applies specifically to Fig. 5c (*RALDH2*; lower panels).

References

- Grocott, T., Tambalo, M. & Streit, A. The peripheral sensory nervous system in the vertebrate head: a gene regulatory perspective. *Dev. Biol.* **370**, 3–23 (2012).
- Saint-Jeannet, J. P. & Moody, S. A. Establishing the pre-placodal region and breaking it into placodes with distinct identities. *Dev. Biol.* **389**, 13–17 (2014).
- Schlosser, G. Making sense development of vertebrate cranial placodes. *Int. Rev. Cell Mol. Biol.* **283**, 129–234 (2010).
- Ahrens, K. & Schlosser, G. Tissues and signals involved in the induction of placodal *Six1* expression in *Xenopus laevis*. *Dev. Biol.* **288**, 40–59 (2005).
- Brugmann, S. A., Pandur, P. D., Kenyon, K. L., Pignoni, F. & Moody, S. A. *Six1* promotes a placodal fate within the lateral neurogenic ectoderm by functioning as both a transcriptional activator and repressor. *Development* **131**, 5871–5881 (2004).
- Litsiou, A., Hanson, S. & Streit, A. A balance of FGF, BMP and WNT signalling positions the future placode territory in the head. *Development* **132**, 4051–4062 (2005).
- Hong, C. S. & Saint-Jeannet, J. P. The activity of *Pax3* and *Zic1* regulates three distinct cell fates at the neural plate border. *Mol. Biol. Cell* **18**, 2192–2202 (2007).
- Kuo, J. S. *et al.* Opl: a zinc finger protein that regulates neural determination and patterning in *Xenopus*. *Development* **125**, 2867–2882 (1998).
- Sato, T., Sasai, N. & Sasai, Y. Neural crest determination by co-activation of *Pax3* and *Zic1* genes in *Xenopus* ectoderm. *Development* **132**, 2355–2363 (2005).
- Monsoro-Burq, A. H., Wang, E. & Harland, R. *Msx1* and *Pax3* cooperate to mediate FGF8 and WNT signals during *Xenopus* neural crest induction. *Dev. Cell* **8**, 167–178 (2005).
- Bae, C. J. *et al.* Identification of *Pax3* and *Zic1* targets in the developing neural crest. *Dev. Biol.* **386**, 473–483 (2014).
- Knecht, A. K., Good, P. J., Dawid, I. B. & Harland, R. M. Dorsal-ventral patterning and differentiation of noggin-induced neural tissue in the absence of mesoderm. *Development* **121**, 1927–1935 (1995).
- Lepperdinger, G., Engel, E. & Richter, K. A retinoid-binding lipocalin, *Xlcp1*, relevant for embryonic pattern formation is expressed in the nervous system of *Xenopus laevis*. *Dev. Genes Evol.* **207**, 177–185 (1997).
- Lepperdinger, G. *et al.* The lipocalin *Xlcp1* expressed in the neural plate of *Xenopus laevis* embryos is a secreted retinaldehyde binding protein. *Protein Sci.* **5**, 1250–1260 (1996).
- Richter, K., Grunz, H. & Dawid, I. B. Gene expression in the embryonic nervous system of *Xenopus laevis*. *Proc. Natl Acad. Sci. USA* **85**, 8086–8090 (1988).
- Mayor, R., Morgan, R. & Sargent, M. G. Induction of the prospective neural crest of *Xenopus*. *Development* **121**, 767–777 (1995).
- Pandur, P. D. & Moody, S. A. *Xenopus Six1* gene is expressed in neurogenic cranial placodes and maintained in the differentiating lateral lines. *Mech. Dev.* **96**, 253–257 (2000).

18. Schlosser, G. & Ahrens, K. Molecular anatomy of placode development in *Xenopus laevis*. *Dev. Biol.* **271**, 439–466 (2004).
19. Pohl, B. S., Knochel, S., Dillinger, K. & Knochel, W. Sequence and expression of FoxB2 (XFD-5) and FoxI1c (XFD-10) in *Xenopus* embryogenesis. *Mech. Dev.* **117**, 283–287 (2002).
20. Mizuseki, K., Kishi, M., Matsui, M., Nakanishi, S. & Sasai, Y. *Xenopus* Zic-related-1 and Sox-2, two factors induced by chordin, have distinct activities in the initiation of neural induction. *Development* **125**, 579–587 (1998).
21. Huang, X., Hong, C. S., O'Donnell, M. & Saint-Jeannet, J. P. The doublesex-related gene, *XDmrt4*, is required for neurogenesis in the olfactory system. *Proc. Natl Acad. Sci. USA* **102**, 11349–11354 (2005).
22. Heller, N. & Brandli, A. W. *Xenopus* Pax-2/5/8 orthologues: novel insights into Pax gene evolution and identification of Pax-8 as the earliest marker for otic and pronephric cell lineages. *Dev. Genet.* **24**, 208–219 (1999).
23. Takabatake, Y., Takabatake, T. & Takeshima, K. Conserved and divergent expression of T-box genes *Tbx2-Tbx5* in *Xenopus*. *Mech. Dev.* **91**, 433–437 (2000).
24. Urade, Y. & Hayaishi, O. Biochemical, structural, genetic, physiological, and pathophysiological features of lipocalin-type prostaglandin D synthase. *Biochim. Biophys. Acta* **1482**, 259–271 (2000).
25. Urade, Y. *et al.* Structural and functional significance of cysteine residues of glutathione-independent prostaglandin D synthase. Identification of Cys65 as an essential thiol. *J. Biol. Chem.* **270**, 1422–1428 (1995).
26. Tanaka, T. *et al.* Lipocalin-type prostaglandin D synthase (beta-trace) is a newly recognized type of retinoid transporter. *J. Biol. Chem.* **272**, 15789–15795 (1997).
27. Minucci, S. *et al.* Retinoid X receptor-selective ligands produce malformations in *Xenopus* embryos. *Proc. Natl Acad. Sci. USA* **93**, 1803–1807 (1996).
28. Chen, Y., Pollet, N., Niehrs, C. & Pieler, T. Increased XRALDH2 activity has a posteriorizing effect on the central nervous system of *Xenopus* embryos. *Mech. Dev.* **101**, 91–103 (2001).
29. Chen, Y. & Reese, D. H. A screen for disruptors of the retinol (vitamin A) signaling pathway. *Birth Defects Res. B Dev. Reprod. Toxicol.* **98**, 276–282 (2013).
30. Strate, I., Min, T. H., Iliev, D. & Pera, E. M. Retinol dehydrogenase 10 is a feedback regulator of retinoic acid signalling during axis formation and patterning of the central nervous system. *Development* **136**, 461–472 (2009).
31. Johnson, A. T. *et al.* Synthesis and characterization of a highly potent and effective antagonist of retinoic acid receptors. *J. Med. Chem.* **38**, 4764–4767 (1995).
32. Koide, T., Downes, M., Chandraratna, R. A. S., Blumberg, B. & Umesono, K. Active repression of RAR signaling is required for head formation. *Genes Dev.* **15**, 2111–2121 (2001).
33. Hernandez, R. E., Rikhof, H. A., Bachmann, R. & Moens, C. B. *vhnfl* integrates global RA patterning and local FGF signals to direct posterior hindbrain development in zebrafish. *Development* **131**, 4511–4520 (2004).
34. Schug, T. T., Berry, D. C., Shaw, N. S., Travis, S. N. & Noy, N. Opposing effects of retinoic acid on cell growth result from alternate activation of two different nuclear receptors. *Cell* **129**, 723–733 (2007).
35. Jetten, J. Retinoid-related orphan receptors (RORs): critical roles in development, immunity, circadian rhythm, and cellular metabolism. *Nucl. Recept. Signal.* **7**, e003 (2009).
36. Stehlin-Gaon, C. *et al.* All-trans retinoic acid is a ligand for the orphan nuclear receptor ROR β . *Nat. Struct. Biol.* **10**, 820–825 (2003).
37. Knecht, A. K. & Harland, R. M. Mechanisms of dorsal-ventral patterning in noggin-induced neural tissue. *Development* **124**, 2477–2488 (1997).
38. Cornish, E. J., Hassan, S. M., Martin, J. D., Li, S. & Merzdorf, C. S. A microarray screen for direct targets of *Zic1* identifies an aquaporin gene, *aqp-3b*, expressed in the neural folds. *Dev. Dyn.* **238**, 1179–1194 (2009).
39. Urade, Y. & Hayaishi, O. Prostaglandin D synthase: structure and function. *Vitam. Horm.* **58**, 89–120 (2000).
40. Shiotsugu, J. *et al.* Multiple points of interaction between retinoic acid and FGF signaling during embryonic axis formation. *Development* **131**, 2653–2667 (2004).
41. Janesick, A., Shiotsugu, J., Taketani, M. & Blumberg, B. *RIPPLY3* is a retinoic acid-inducible repressor required for setting the borders of the pre-placodal ectoderm. *Development* **139**, 1213–1224 (2012).
42. Cammas, L. *et al.* Retinoic acid receptor (RAR)- α is not critically required for mediating retinoic acid effects in the developing mouse retina. *Invest. Ophthalmol. Vis. Sci.* **51**, 3281–3290 (2010).
43. Duester, G. Retinoic acid synthesis and signaling during early organogenesis. *Cell* **134**, 921–931 (2008).
44. Kam, R. K., Deng, Y., Chen, Y. & Zhao, H. Retinoic acid synthesis and functions in early embryonic development. *Cell Biosci.* **2**, 11 (2012).
45. Rhinn, M. & Dolle, P. Retinoic acid signalling during development. *Development* **139**, 843–858 (2012).
46. Wu, J., Yang, J. & Klein, P. S. Neural crest induction by the canonical Wnt pathway can be dissociated from anterior-posterior neural patterning in *Xenopus*. *Dev. Biol.* **279**, 220–232 (2005).
47. Mandal, A. *et al.* Transgenic retinoic acid sensor lines in zebrafish indicate regions of available embryonic retinoic acid. *Dev. Dyn.* **242**, 989–1000 (2013).
48. Ribes, V., Wang, Z., Dolle, P. & Niederreither, K. Retinaldehyde dehydrogenase 2 (RALDH2)-mediated retinoic acid synthesis regulates early mouse embryonic forebrain development by controlling FGF and sonic hedgehog signaling. *Development* **133**, 351–361 (2006).
49. Blentic, A., Gale, E. & Maden, M. Retinoic acid signalling centres in the avian embryo identified by sites of expression of synthesising and catabolising enzymes. *Dev. Dyn.* **227**, 114–127 (2003).
50. Maden, M., Gale, E., Kostetskii, I. & Zile, M. Vitamin A-deficient quail embryos have half a hindbrain and other neural defects. *Curr. Biol.* **6**, 417–426 (1996).
51. Maden, M. *et al.* Retinoic acid is required for specification of the ventral eye field and for Rathke's pouch in the avian embryo. *Int. J. Dev. Biol.* **51**, 191–200 (2007).
52. Lee, L. M. *et al.* A paradoxical teratogenic mechanism for retinoic acid. *Proc. Natl Acad. Sci. USA* **109**, 13668–13673 (2012).
53. Tanibe, M. *et al.* Retinoic acid metabolizing factor *xCyp26c* is specifically expressed in neuroectoderm and regulates anterior neural patterning in *Xenopus laevis*. *Int. J. Dev. Biol.* **52**, 893–901 (2008).
54. Drummond, D. L. *et al.* The role of *Zic* transcription factors in regulating hindbrain retinoic acid signaling. *BMC Dev. Biol.* **13**, 13–31 (2013).
55. Maurus, D. & Harris, W. A. *Zic*-associated holoprosencephaly: zebrafish *Zic1* controls midline formation and forebrain patterning by regulating Nodal, Hedgehog, and retinoic acid signaling. *Genes Dev.* **23**, 1461–1473 (2009).
56. Kolm, P. J. & Sive, H. L. Efficient hormone-inducible protein function in *Xenopus laevis*. *Dev. Biol.* **171**, 267–272 (1995).
57. Nieuwkoop, P. D. & Faber, J. *Normal Table of Xenopus laevis* (North Holland Publishing Company, 1967).
58. Slack, J. M. & Forman, D. An interaction between dorsal and ventral regions of the marginal zone in early amphibian embryos. *J. Embryol. Exp. Morphol.* **56**, 283–299 (1980).
59. Harland, R. M. In situ hybridization: an improved whole-mount method for *Xenopus* embryos. *Methods Cell Biol.* **36**, 685–695 (1991).
60. Henry, G. L., Brivanlou, I. H., Kessler, D. S., Hemmati-Brivanlou, A. & Melton, D. A. TGF- β signals and a pattern in *Xenopus laevis* endodermal development. *Development* **122**, 1007–1015 (1996).

Acknowledgements

We are grateful to Dr Yoshihiro Urade, Dr Ko Fujimori and Dr Edgar Pera for reagents, Dr John Tobias for help with the microarray data and Dr Jane McCutcheon for comments on the manuscript. We thank Dr Juhee Jeong and members of the Jeong laboratory for discussions.

Author contributions

M.B.J. and J.-P.S.-J. designed the experiments and wrote the manuscript. M.B.J., H.J.-G., A.D. and J.-P.S.-J. performed the experiments and analysed the data. M.B.J., H.J.-G. and J.-P.S.-J. prepared the figures. All authors have read and approved the final manuscript. This work was funded by a grant from the National Institutes of Health to J.-P.S.-J. (R01-DE014212).

Additional information

Accession codes: The microarray data have been deposited in the GEO database under the accession number GSE68546.

Supplementary Information accompanies this paper at <http://www.nature.com/naturecommunications>

Competing financial interests: The authors declare no competing financial interests.

Reprints and permission information is available online at <http://npg.nature.com/reprintsandpermissions/>

How to cite this article: Jaurena, M. B. *et al.* *Zic1* controls placode progenitor formation non-cell autonomously by regulating retinoic acid production and transport. *Nat. Commun.* 6:7476 doi: 10.1038/ncomms8476 (2015).